



Synthesis, characterization and inhibitory activity against breast carcinoma cells of a new Azo-Ligand and its Metal complexes

Ali M. Hassan^a, Bassem H. Heikal^{b*}, Tamer M. Kehela^c, O. A. Fouad^d and A. Mohy Eldin^e

^aChemistry Dept., Faculty of Science, Al-Azhar University, Nasr City, Cairo, Egypt

^bResearch and Development, Cairo Oil Refining Company, Cairo, Egypt

^cForensic medicine authority, Ministry of Justice, Cairo, Egypt

^dCentral Metallurgical Research & Development Institute, Helwan, Cairo, Egypt

^eResearch and Development, Bachin Painting Co., Cairo, Egypt

ABSTRACT

A novel azopyrimidin ligand *N*-(1-(4-aminophenyl)ethylidene)-4-(2-amino-3-(4-methoxyphenyl)diazenyl)[1,5-*a*]pyrimidin-7-yl)benzeneamine. The prepared azo-ligand was used for further complexes formation reaction with different metal ions using Ni(II)(CH₃COO)₂, Cu(II)(CH₃COO)₂, Pd(II)Cl₂, Ag(I)NO₃, Pt(IV)Cl₄ and HAu(III)Cl₄ by a molar ratio of ligand : metals. The stereochemistry and the mode of bonding of the complexes were achieved based on elemental analysis, IR, UV-Vis, ¹HNMR and MS as well as thermo-gravimetric analysis (TGA). Structures proposed for geometry of the chelates based on their electronic spectra and magnetic moment. The metal complexes possessed an tetrahedral for [Ni(II) and Cu(II)], square planer for [Pd(II), Pt(IV) and Au(III)] and a trigonal geometry for Ag(I). The solid complexes have been synthesized and studied by TGA analysis. The thermal dehydration and decomposition of these complexes were studied kinetically using the integral method applying the Coats-Redfern and Horowitz Metzger equation. The band gap energy values of all compounds are characteristic of semiconductor materials. The metal complexes show inhibitory activity against breast carcinoma cells.

Keywords: Azo pyrimidine, Breast cancer, Thermal kinetics; Band gap Energy

INTRODUCTION

Azo-compounds play an important role in analytical chemistry as metal chromogenic agents [1], in industrial dyes [2], acid-base indicators as well as uses as histological stains [3]. Also some azo-compounds possess excellent optical memory and photoelectric properties [4]. Various studies have been done on the aryl azo heterocyclic and their metal complexes [5]. The pyrimidine compounds are one of the important classes, so several studies were reported on the structural chemistry of the pyrimidine compounds and their metal complexes [6]. In view of these finding and in continuation to our work on the spectral behavior of azo-dyes and their metal complexes [7]. Schiff bases, products of the reaction of primary amines and carbonyl compounds, are involved in many metabolic processes. Numerous products of further fragmentation and cross-linking are responsible for the color, flavor, and taste of foods and drinks [8]. Salicyliden- and 2-hydroxynaphthylideneamines have been the subject of particular interest because some of their complexes are found in nature and biological activities have been recorded for the synthesized ones [9]. Pyrimidine is the parent heterocycle of a very important group of compounds that have been extensively studied due to their occurrence in living systems [10]. Pyrimidines are reported to have a broad spectrum of biological activities. Some are endowed with antitumor [11], antiviral [12], antiinflammatory [13], antipyretic [14], antimicrobial [15] and antifungal [16] properties. Considerable attention has been given to the metal(II) complexes of polydentate Schiff base ligands of the *N*-aminopyrimidine type, due to their structural richness and electrochemical properties as well as their potential as a model for a number of important biological systems [17, 18]. New organic materials have attracted much attention over recent years for their light-emitting properties [19-

21]. For example, organic polymers that exhibit strong luminescence at low driving voltages, particularly those that emit in the blue region, are of great interest for flat panel display applications [22, 23]. Rare earth complexes with low-molecular-weight organic ligands have also been extensively studied to obtain highly fluorescent materials for application in electroluminescent devices [24, 25] and laser systems [26]. The design and testing of gold complexes as antitumour agents derives from several facts [27-32]. Additionally some gold(III) complexes present a good stability in aqueous and physiological environments [33], however, due to the high reduction potential of gold(III), this is not a general rule. Considerable attention has been given to metal(II) complexes of the polydentate Schiff base ligands of N-aminopyrimidine because of their bioinorganic relevance, which has often been related to their chelating ability with trace metal ions [34-37]. Recent findings of the presence of metal-sulfur and metal-nitrogen bonds at the active sites of several oxidoreductases have stimulated an immense amount of interest in pyrimidine chemistry [38, 39].

In view of the significant structural and biological applications of pyrimidine compound as (N-(1-(4-aminophenyl)ethylidene)-4-(2-amino-3-(4-methoxyphenyl)diazenyl)-[1,5-a]pyrimidin-7-yl)benzeneamine and their Nickel(II), Copper(II), Palladium(II), Silver(I), Platinum(IV) and Gold(III) metal complexes 1-6 (Scheme 1). These compounds have been investigated for inhibitory activity against breast carcinoma cells.

EXPERIMENTAL SECTION

2.1. Materials and physical methods:

The selected metal salts were purchased from Sigma-Aldrich. The aldehydes were of E-Merck grade. Other chemicals and solvents were of highest purity and used without further purification. Melting points were recorded on a Griffine Gearge melting point apparatus. The electronic absorption spectra were recorded in DMSO from 900-200 nm using Perkin Elmer Lambda 35 UV/Vis spectrometer, fitted with a quartz cell of 1.0 cm path length. The Fourier transform infrared spectra with the samples in KBr were recorded on Perkin-Elmer Spectrophotometer, USA from 4000-400 cm^{-1} . The elemental analysis (C, H and N) are carried out using a Perkin-Elmer USA model. The ^1H NMR spectra were recorded in DMSO- d_6 using TMS as internal standard on a Jeol-FX-90Q Fourier NMR spectrometer. Thermal analysis measurements were carried out on Shimadzu TGA. Mass spectra were performed by a Shimadzu-GC-MS-QP1000 EX using the direct inlet system. Metals (Ni, Cu, Pd, Ag and Pt) were determined by complexometric titration using xylenol orange (XO) as indicator and hexamine as buffer (pH = 6) [40] except the Au metal was determined by (ICP MS 7700x agilent). Antitumor evaluation, read the absorbance at 490 nm using ELISA reader (SunRise, TECAN, INC, USA) were studied at Al-Azhar University, Cairo; Egypt. Magnetic Susceptibility of prepared complexes was measured in micro analytical laboratory of faculty of Science Cairo University, Giza, Egypt. The ESR spectra of the powdered Cu (II) and Au(III) samples were carried out on Bruker-EMX-(Xbands-9.7 GHz) spectrometer with 100 KHZ frequency, microwave power 1.008 MW and modulation/amplitude of 4 GAUSS at national center for radiation research and technology, Egypt. The optical band gap energy (E_g) of product compounds was calculated from Tuac's equations.

2.2. Preparation

2.2.1. Preparation of ligand (L)

The ligand was prepared as described in the literature [41] with minor modifications in the purification procedure and the characterization results completely agreed with the reported data. The physical, analytical and spectral data is given in Tables 1 and 2.

N-(1-(4-aminophenyl)ethylidene)-4-(2-amino-3-(4-ethoxyphenyl)diazenyl)[1,5-a]pyrimidin-7-yl)benzeneamine: Brown color. Elemental analysis for $\text{C}_{27}\text{H}_{24}\text{N}_8\text{O}$: C % (calc., 68.05 ; found; 68.23), H % (calc., 5.08 ; found, 5.14) and N % (calc., 23.51 ; found, 23.42). m.p: 200 $^{\circ}\text{C}$. ESI-MS: $m/z = 476$, $\text{C}_{27}\text{H}_{24}\text{N}_8\text{O}$, where calculated $m/z = 476.2$.

2.2.2. Preparation of solid complexes

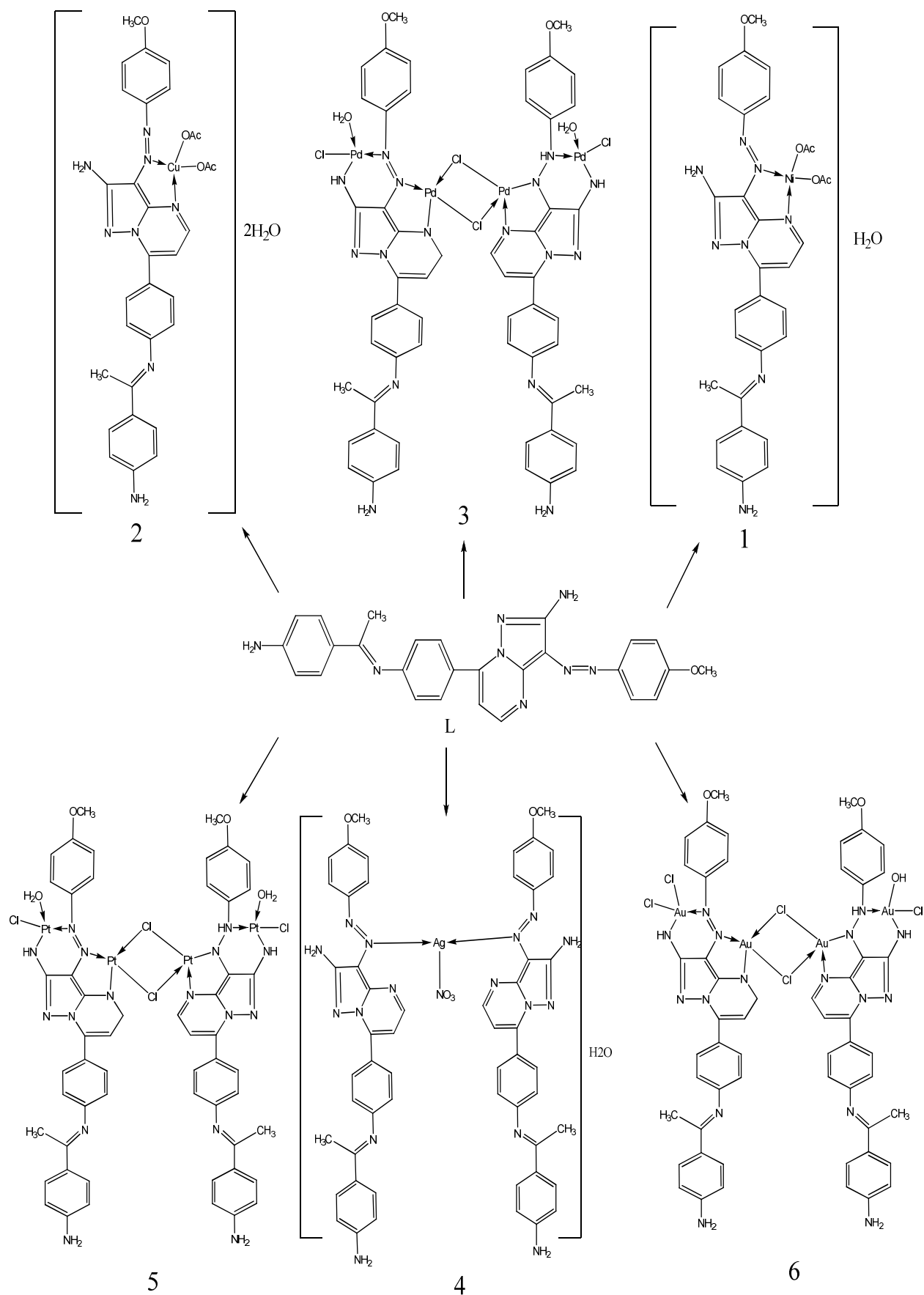
Preparation of $\text{Ni}(\text{CH}_3\text{COOH})_2 \cdot 4\text{H}_2\text{O}$ (104 mg, 0.418 mmol), $\text{Cu}(\text{CH}_3\text{COOH})_2 \cdot \text{H}_2\text{O}$ (86.44 mg, 0.417 mmol), PdCl_2 (37 mg, 0.20867 mmol) was added to 3.7 mg of NaCl and grinding the mixture), AgNO_3 (71.04 mg, 0.418 mmol), PtCl_4 (70 mg, 0.209 mmol) and $\text{H}[\text{AuCl}_4]$ (71 mg, 0.209 mmol) with N-(1-(4-aminophenyl)ethylidene)-4-(2-amino-3-(4-methoxyphenyl)-diazen-yl)[1,5-a] pyrimidin-7-yl)benzeneamine (L) (100 mg, 0.20896 mmol). A hot ethanol solution (20 ml) of Ni(II), Cu(II), Pd(II), Ag(I), Pt(IV) and Au(III) was added dropwise to a magnetically stirred solution of the ligand (L) in ethanol (25 ml). The resultant mixture was refluxed for 3 hrs. During refluxing a solid product precipitated out which was filtered, washed with ethanol and then with diethyl ether and dried. The preparation of complexes (Scheme 1). Physical, analytical and spectral data is given in Tables 1 and 2.

2.3. Methods of anti-tumor evaluation

Human breast cancer (MCF-7) cells were obtained from the American type culture collection (ATCC, ROCKVILLE, MD). The cells were grown on RPMI-1640 medium supplemented with 10 % inactivated fetal calf serum and 50 µg/ml gentamycin. The cells were maintained at 37 °C in a humidified atmosphere with 5 % CO₂ and were subcultures two to three times a week. The anti-tumor activity was evaluated on MCF-7 cells. The cells were grown as monolayer in growth RPMI-1640 medium supplemented with 10 % inactivated fetal calf serum and 50 µg/ml gentamycin. The monolayer of 10,000 cells adhered at the bottom of the wells in a 96-well microtiter plate incubated for 24 hrs at 37 °C in a humidified incubator with 5 % CO₂. The monolayer were then washed with sterile phosphate buffered saline (0.01 M, pH 7.2) and simultaneously the cells were treated with 100 µl from different dilutions of the test sample in fresh maintenance medium and incubated at 37 °C. A control of untreated cells was made in the absence of the test sample. Six wells were used for each concentration of the test sample. Every 24 hrs the observation under the inverted microscope was made. The number of the surviving cells was determined by staining the cells with crystal violet [42] followed by the cell lysine using 33 % glacial acetic acid and read the absorbance at 490 nm using ELISA reader (SunRise, TECAN, INC, USA) after well mixing. The absorbance values from untreated cells were considered as 100 % proliferation. The number of viable cells was determined using ELISA reader as previously mentioned before and the percentage of viability was calculated as $[1-(OD_t/OD_c)] \times 100$ % where OD_t is the mean optical density of wells treated with the test sample and OD_c is the mean optical density of the untreated cells. The 50 % inhibitory concentration (IC₅₀) was estimated from graphic plots.

Table 1: Analytical, physical and spectroscopic data of the azo ligand (L) and their related metal complexes

Molecular Formula	Symbol	M.P °C	Color	Elemental Analysis				¹ H-NMR Chemical shift (δppm)	μ _{eff}	M ⁺ Calc./ (Found)	E _g (eV)
				C	H	N	M				
C ₂₇ H ₂₄ N ₈ O	L	200	Brown	68.05 (68.23)	5.08 (5.14)	23.51 (23.42)	-	δ2.5 (dd, 1H, CH ₃ J=4.7, 9.8 HZ), δ 3.83 (dd, 1H, OCH ₃ ; J=4.8, 11.8 HZ), δ 7.04 (m, 11H, ArH's), δ 8.54 (s, 1H, azomethine C-H), δ 10.24,10.6 (s,4H,3NH ₂)	-	476.2 (476)	2.72
[Ni(L).(2AcO)]. H ₂ O	1	>300	Deep Brown	55.46 (55.29)	4.80 (4.75)	16.69 (16.51)	8.74 (8.60)	-	2.36	670.13 (669.9)	2.60
[Cu(L).(2AcO)].2H ₂ O	2	>300	Deep Brown	53.63 (52.91)	4.94 (5.1)	16.14 (16.62)	9.15 (9.77)	-	1.85	693.18	2.48
[4Pd(L- 1H) ₂ 4Cl(2H ₂ O)]	3	>300	Deep Red	41.67 (41.47)	3.37 (3.38)	14.40 (14.68)	27.35 (27.28)	-	D	1552 (>1000)	2.53
C ₅₄ H ₅₂ O ₄ N ₁₆ Cl ₄ Pd ₄											
[Ag(NO ₃)(L) ₂].H ₂ O	4	181	Deep Brown	56.85 (57.14)	4.42 (4.87)	20.87 (20.86)	9.45 (8.90)	-	D	1140.9 (>1000)	2.54
C ₅₄ H ₅₀ O ₆ N ₁₇ Ag											
[4Pt(L-H) ₂ 2H ₂ O.4Cl]	5	>300	Reddish Brown	33.94 (33.72)	2.74 (2.43)	11.73 (11.52)	40.83 (40.97)	-	D	1911.2 (>1000)	2.56
C ₅₄ H ₅₂ Cl ₄ N ₁₆ O ₄ Pt ₄											
[4Au(L- 1H) ₂ (OH).5Cl]	6	224	Deep brown	33.51 (33.24)	2.55 (2.75)	11.58 (11.21)	40.71 (40.96)	-	D	1935.2 (>1000)	2.54
C ₅₄ H ₄₉ O ₃ N ₁₆ Cl ₅ Au ₄											



Scheme 1: Ligand and metal complexes

RESULTS AND DISCUSSION

The azo ligand (L) and their solid complexes with metal have been isolated in pure form as (Scheme 1). Physical, analytical and spectroscopic data of the ligand (L) and their isolated complexes are given in (Table 1, 2). Comparison of the elemental analysis for both the calculated and found percentages indicates that the compositions of the isolated solid complexes coincide well with the proposed formula. Also the structure of the solid complexes has been identified on the basis of FT-IR, magnetism and UV-Vis. Spectra. The solvent content of the complexes was determined by thermal TGA measurements and the results can be taken as evidence for the suggested structure.

3.1. IR spectra:

The infrared spectra of the azo-ligand (L) and its metal complexes obtained as KBr discs in the region of 4000 – 400 cm^{-1} and given in the Table 2.

The $\nu(\text{N}=\text{N})$ frequency of the ligand (L) appears at 1503 cm^{-1} , negative shift of the spectra of the complexes take place suggests coordination of one nitrogen of azo group in complexation with metal ions [41,43]. The $\nu(\text{C}=\text{N})$ observed at 1604 cm^{-1} for (L) shift to a lower value occurred in the complexes of (L) due to the participation of N-atom of azo methine in chelation [43]. A broad bands in the 3432 – 3418 cm^{-1} appeared in the spectra of the complexes. The far infrared region shows bands in the range (423 – 470) cm^{-1} assigned to $\nu(\text{M}-\text{N})$ [44].

Table 2: IR spectral and Electronic absorption data of ligand and metal complexes:

Symbol	$\nu(\text{H}_2\text{O})$	$\nu(\text{NH}_2)$ Assym./ Sym.	$\nu(\text{C}-\text{H})$ aromatic aliphatic	$\nu(\text{C}=\text{N})$	$\nu(\text{N}=\text{N})$	$\nu(\text{acetate})$ Sym./ Assym.	$\nu(\text{M}-\text{N})$	$\lambda_{\text{max, nm}}$ (assignments)	Structure
L	-	3277 3186	2932 2839	1604	1503	-	-	390($n-\pi^*$, C=N), 255($\pi-\pi^*$, Phenyl)	-
1	3432	3270 3180	2929 2845	1603	1497	1420 1315	423	539 (${}^3\text{A}_{2g} \rightarrow {}^1\text{E}_g$)	Tetrahedral
2	3418	3281 3179	2966 2882	1593	1490	1418 1316	470	520 (${}^2\text{B}_2 \rightarrow {}^2\text{E}$)	Tetrahedral
3	3417	3320 3214	2926 2845	1601	1490	-	446	L \rightarrow MCT	Square Planar
4	3421	3312 3181	2932 2837	1600	1495	-	431	L \rightarrow MCT	Trigonal
5	3426	3318 3163	2923 2841	1603	1489	-	452	L \rightarrow MCT	Square Planar
6	-	3312 3150	2928 2849	1599	1487	-	470	L \rightarrow MCT	Square Planar

3.2. UV-VIS spectra:

The electronic spectral values of complexes are recorded in Table 2. The electronic spectra of Ni(II) and Cu(II) complexes energy absorption bands at 539 and 520 assigned to the transitions (${}^3\text{A}_{2g} \rightarrow {}^1\text{E}_g$) and (${}^2\text{B}_2 \rightarrow {}^2\text{E}$). On the basis of which a tetrahedral geometry is suggested for Ni(II) and Cu(II) complexes[45]. The diamagnetic of Pd(II), Ag(I), Pt(IV) and Au(III) complexes possess square planar except the silver is a trigonal geometry. The diamagnetic of Ag(I) complex possesses trigonal geometry and chelate show intense absorption in UV-region at a single band in the 352-372 nm region, assigned to charge transfer band, in accord with the $4d^{10}$ to $5s^0$ electronic configuration of silver ion [46]. The electronic spectra of the Pd(II) and Pt(II) complexes had bands in the range of 231-311 nm due to the $n-\pi^*$ and $\pi-\pi^*$ transitions of phenyl, pyrimidine, and azomethine. In the spectra of the complexes, the less intense and broad bands in the range of 311-481 nm resulted from the overlap of the low energy $\pi \rightarrow \pi^*$ transitions, mainly localized within the azomethine group, and the LMCT transitions from the lone pairs of the phenolate oxygen donor to Pd(II) and Pt(II) [47]. The electronic spectra of Au(III) complex gave the absorption band at the range 330 nm, these bands can be assigned to ${}^1\text{A}_{1g} \rightarrow {}^1\text{E}_g$ transition. The position of these bands are in agreement with low-spin square planar geometry for Au(III) complexes [48]. Bands at values higher than 300 nm were assigned to charge transfer. The determined magnetic moment (B.M) values of Nickel and Copper ion metal complexes at room temperature were recorded in Table 1. The magnetic moment values of the Nickel(II) and copper(II) complexes are 2.36 and 1.85 B.M at 298 K.

3.3. Mass spectra of solid metal complexes:

The mass spectral data and fragmentation pattern of the complexes clearly justify [49, 50]. The formation of Ni(II) complex further evidenced by mass spectral data. The proposed molecular formula of these complexes was confirmed by the mass spectral analysis by comparing its molecular formula weight with m/e values. The complexes of Pd(II), Pt(IV) and Au(III) show different m/e values with different intensities. The molecular ion peaks of these complexes not observed due to its high molecular weight than the scale of the mass device, the base peaks of these

complexes observed at m/e 60 for $C_2H_4O_2$, 98 for $C_5H_{10}N_2$, 82 for $C_3H_4N_3$ and are respectively and metal ion peaks at $m/e = 107, 195$ and 197 are respectively as shown in Fig 1.

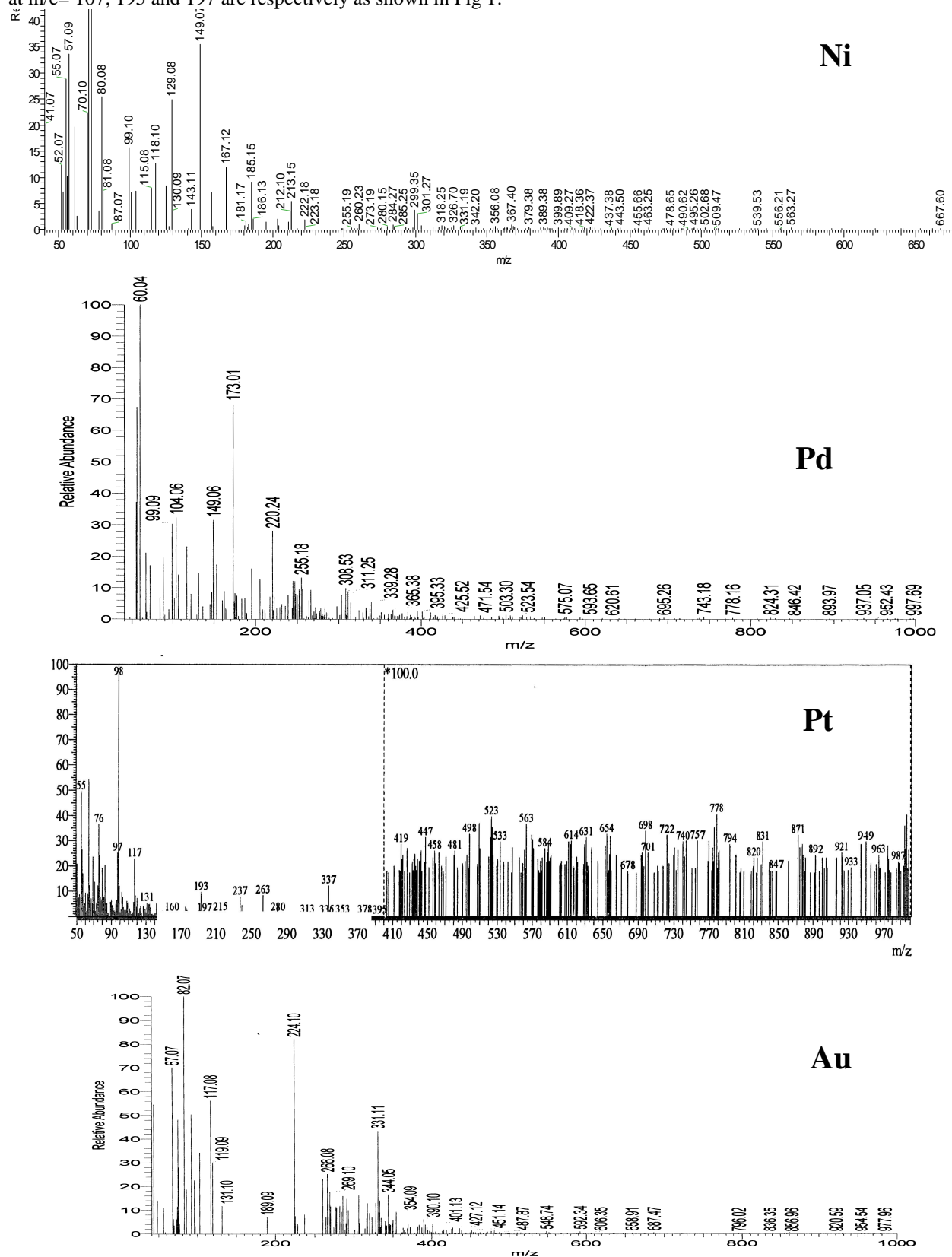


Fig. 1 : Mass spectra of metal complexes (Ni, Pd, Pt and Au)

3.4. $^1\text{H NMR}$ (DMSO- d_6) of L :

The $^1\text{H NMR}$ signals of the azo-ligand (L) are δ 2.5 (dd, 1H, CH_3 $J=4.7, 9.8$ HZ), 3.83 (dd, 1H, OCH_3 $J=4.8, 11.8$ HZ), 7.04 (m, 11H, ArH's), 8.54 (s, 1H, azomethine C-H), 10.24, 10.6 (s, 4H, 2NH_2) [51] Fig. 2.

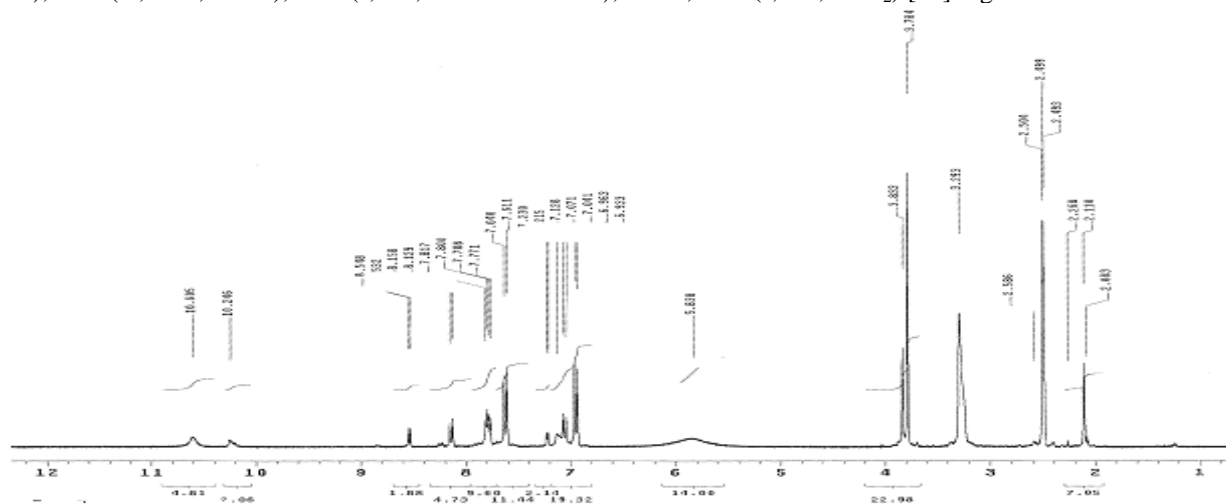
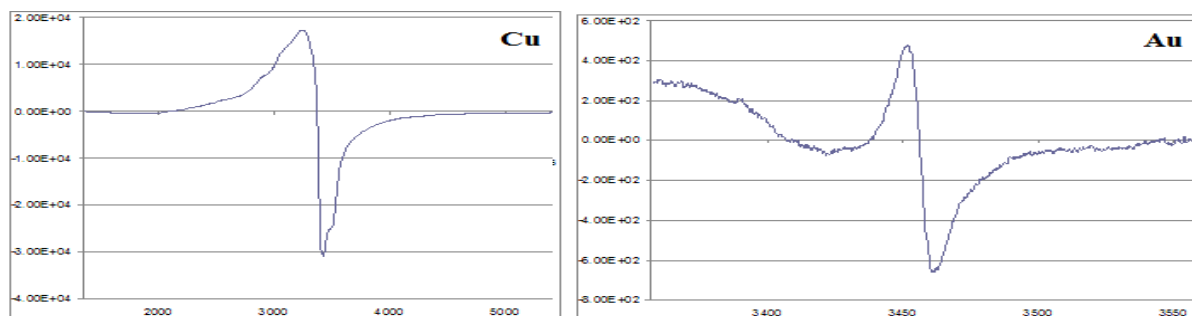


Fig. 2: $^1\text{H NMR}$ spectrum (DMSO- d_6) of Ligand

3.5. ESR Spectra :

The ESR spectra of Cu (II) of L complex were recorded on X-Band at frequency (9.7) GHz under the magnetic field strength (3480) G , recorded at room temperature. The spectra of the complexes exhibit a single anisotropic broad signal. From Fig. 3 this anisotropic spectrum of ESR of Cu (II) shows a $g_{\perp} > g_{\parallel}$ with the following values $g_{\parallel} = 2.00545$ and $g_{\perp} = 2.13601$ in which $g_{\perp} > g_{\parallel} > 2.0023$ calculated for Cu (II) complex, suggest that the unpaired electron is localized in $d_{x^2-y^2}$ orbital $g_{\perp} > g_{\parallel}$. These values indicate that the ground state of Cu (II) is predominately $d_{x^2-y^2}$, which suppose a tetrahedral .The observed g_{\parallel} value for Cu (II) complex is less than 2.3, thus, indicating the bonds between the organic ligand and copper ion have a covalent character more than the ionic character [52].

The EPR spectrum of Au (III) complex shows axial signals shape and having symmetric bands with two g values, $g_{\parallel} = 2.0096$ and $g_{\perp} = 2.01256$. These values suggest a square planner stereochemistry for the complex. The geometric structure with $g_{\parallel} < g_{\perp}$ indicates that the electron is delocalized in d_{z^2} orbital of the ground state of Au(III) ion. The g_{\parallel} is an important function for indicating covalent character of M-L bond [53, 54]. For ionic character of the nuclei ligand bond, $g_{\parallel} > 2.3$ and for covalent environment $g_{\parallel} < 2.3$. In this Au (III) complex $g_{\parallel} < 2.3$ was obtained. This indicates an appreciable covalent character in the Au-L bond Fig 3.



Figs. 3: ESR spectra of Cu(II) and Au (III) complexes

3.6. Thermal analysis of metal complexes:

In the present investigation, the heating rates were suitably controlled at $10\text{ }^{\circ}\text{C min}^{-1}$ under nitrogen atmosphere and the weight loss was measured from ambient temperature up to $30\text{-}900\text{ }^{\circ}\text{C}$. The TGA data of the thermal decomposition of the complexes are shown in Table 3, Fig. 4. The thermogram of $[\text{Cu}(\text{L})(2\text{AcO})] \cdot 2\text{H}_2\text{O}$, $[\text{4Pd}(\text{L}-\text{1H})_2 \cdot 4\text{Cl}(2\text{H}_2\text{O})]$, $[\text{Ag}(\text{NO}_3)(\text{L})_2] \cdot \text{H}_2\text{O}$, $[\text{4Pt}(\text{L}-\text{H})_2 \cdot 2\text{H}_2\text{O} \cdot 4\text{Cl}]$, $[\text{4Au}(\text{L}-\text{1H})_2(\text{OH}) \cdot 5\text{Cl}]$ and chelates show decomposition steps within the temperature range $30\text{-}900\text{ }^{\circ}\text{C}$, respectively. The first step of decomposition within the temperature ranges ($77\text{-}124$, $39\text{-}132$, $30\text{-}112$) $^{\circ}\text{C}$ corresponds to the loss of $2\text{H}_2\text{O}$ (5.19 %, 2.3 % and 1.88 %) in Cu, Pd and Pt are respectively, Ag (33-170) loss of (H_2O , HNO_3) (7.09 %) and Au (36-141) loss of ($5\text{HCl} + \text{H}_2\text{O}$), (10.23 %) molecules of complexes. The second step of decomposition within temperature ranges ($124\text{-}243$, $132\text{-}280$, $170\text{-}330$, $121\text{-}288$ and $142\text{-}264$) $^{\circ}\text{C}$ corresponds to the loss of acetate (2AcO) (17.01 %), 4HCl (9.37%),

($C_{30}H_{31}N_4O_2$) (42.03%), 4HCl (7.63%) and $C_{16}H_{18}N_4$ (13.6 %) molecules mass loss Of (Cu, Pd, Ag, Pt and Au) are respectively. Third step of decomposition step within temperature ranges (243-269, 280-731, 330-549, 288-477 and 264-325) °C corresponds to the loss of organic molecule with molecular formula C_7H_7NO (17.45%), $C_{54}H_{48}N_{16}O_2$ (61.22 %), $C_{24}H_{26}N_{12}$ (41.40%), $C_{16}H_{18}N_4$ (13.93%) and $C_{14}H_{14}O_2$ (10.93%) of molecules mass loss Of (Cu, Pd, Ag, Pt and Au) are respectively. The fourth step of decomposition step within temperature ranges (270-365, 477-564 and 325-537) °C corresponds to the loss of organic molecule with molecular formula C_8H_9N (17.16 %), $C_{38}H_{34}N_{12}O_2$ (36.14 %) and $C_{12}H_8$ (7.76 %) of molecules mass loss Of (Cu, Pt and Au) are respectively. And the fifth step of decomposition step within temperature range (366-489, 537-685) °C corresponds to the loss of organic molecule with molecular formula $C_{12}H_8N_6$ (34.02 %) and $C_{12}H_{12}N_{12}$ (16.56 %) of molecules mass loss Of (Cu and Au) are respectively. The ligand leaving metal oxide as a residue of (Cu, Pd, Ag, Pt and Au) as shown in Fig. 4 and Table 3. The thermodynamic activation parameters of decomposition processes of dehydrated complexes namely activation energy (E^*), enthalpy (ΔH^*), entropy (ΔS^*) and Gibbs free energy change of the decomposition (ΔG^*) are evaluated graphically by employing the Coats–Redfern relation [55] and Horowitz-Metzger [56]. Kinetic parameters for the first stages, calculated by employing the Coats-Redfern and Horowitz-Metzger equations, are summarized in Table 4, together with the radii of metal ions. The results show that the values obtained by various methods are comparable. The kinetic data obtained with the two methods are in harmony with each other. The activation energy of Cu(II), Pd(II), Ag(I), Pt(IV) and Au(III) complexes expected to increase in relation with decrease in their radius. All the complexes have the square-planar except the silver trigonal geometry and nickel and copper tetrahedral geometry and similar decomposition steps. The smaller size of the ions permits a closer approach of the ligand. Hence the E^* value in the fourth stages for the Pt(IV) complex is higher than for the other complexes. The entropy of activation (ΔS^*), enthalpy of activation (ΔH^*) and the free energy change of activation (ΔG^*) were calculated. The data are summarized in Table 4. The high values of the activation energies reflect the thermal stability of the complexes. The negative values indicate that the activated complexes have a more ordered structures than the reactants and that the complication reactions are slower than the normal [57, 58].

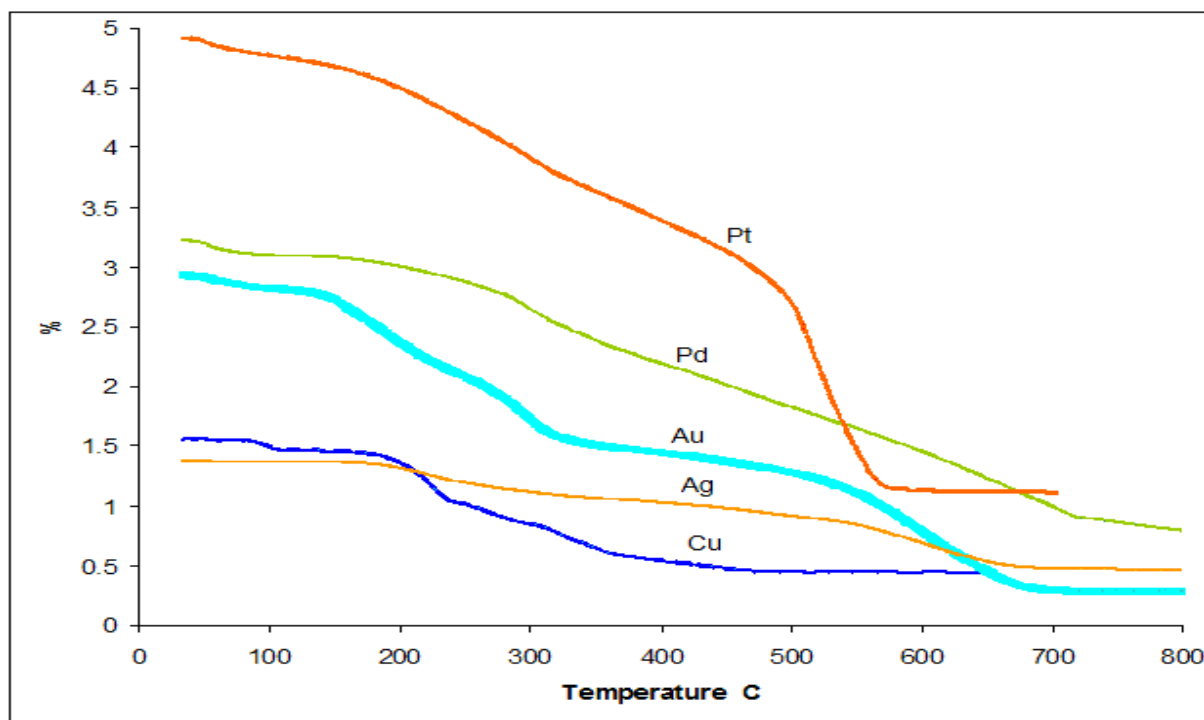


Fig. 4: Thermal decomposition of Cu, Pd, Ag, Pt and Au complexes

Table (3) : Thermal decomposition of Cu, pd, Ag, Pt and Au complexes

Compd. No.	Molecular Formula	Molecular Weight	Steps	ΔT °C		mass %	Assignment
				T_i	T_f		
2	$C_{31}H_{34}CuN_8O_7$	694.2	1st	77	124	5.19	2H ₂ O
			2nd	124	243	17.01	2CH ₃ COO
			3rd	243	269	17.45	C ₇ H ₇ NO
			4th	270	365	17.16	C ₈ H ₉ N
			5th	366	489	34.02	C ₁₂ H ₈ N ₆
			Residue			9.15	CuO
3	$C_{54}H_{52}Cl_4N_{16}O_4Pd_4$	1556.59	1st	39	132	2.30	2H ₂ O
			2nd	132	280	9.37	4HCl
			3rd	280	731	61.22	C ₅₄ H ₄₈ N ₁₆ O ₂
			Residue			27.34	4PdO
4	$C_{54}H_{50}AgN_{17}O_6$	1140.95	1st	33	170	7.09	H ₂ O, HNO ₃
			2nd	170	330	42.03	C ₃₀ H ₃₄ N ₄ O ₂
			3rd	330	549	41.40	C ₂₄ H ₂₆ N ₁₂
			Residue			10.85	AgO
5	$C_{54}H_{52}Cl_4N_{16}O_4Pt_4$	1911.22	1st	30	112	1.88	2H ₂ O
			2nd	121	288	7.63	4HCl
			3rd	288	477	13.93	C ₁₆ H ₁₈ N ₄
			4th	477	564	36.14	C ₃₈ H ₃₄ N ₁₂ O ₂
			Residue			40.82	4PtO
6	$C_{54}H_{49}Au_4Cl_5N_{16}O_3$	1935.2	1st	36	141	10.23	5HCl, H ₂ O
			2nd	142	264	14.25	C ₁₆ H ₁₈ N ₄
			3rd	264	325	10.93	C ₁₄ H ₁₄ O ₂
			4th	325	537	7.76	C ₁₂ H ₈
			5th	537	685	16.56	C ₁₂ H ₁₂ N ₁₂
Residue			40.70	4AuO			

Table 4: Kinetics data of the Cu, pd, Ag, Pt and Au complexes

Compd No.	Steps	Coats Redfern						Horowitz-Metzger					
		R ²	E _a KJ mol ⁻¹	A S ⁻¹	ΔS^* mol ⁻¹ K ⁻¹	ΔH^* KJ mol ⁻¹	ΔG^* KJ mol ⁻¹	R ²	E _a KJ mol ⁻¹	A S ⁻¹	ΔS^* mol ⁻¹ K ⁻¹	ΔH^* KJ mol ⁻¹	ΔG^* KJ mol ⁻¹
2	1 st	0.98	110.5	9.4x10 ¹⁴	39.8	10.7	96	0.98	50.8	5.8x10 ⁶	-147.7	47.7	102.7
	2 nd	0.99	181.2	5.8x10 ¹⁰	-99.7	177	227	0.99	11	1.3x10 ¹¹	-41.9	105.6	126.7
	3 rd	0.99	368.4	2.8x10 ²⁶	31.2	363.9	347	0.99	175	6.5x10 ¹⁶	53.6	170.8	141.8
	4 th	0.98	97.7	3.9x10 ⁷	110.5	92.7	159	0.98	48	2.3x10 ³	-191.8	42.9	158
	5 th	0.96	108.3	1x10 ⁷	-131.3	102.5	194	0.96	52	9.9x10 ²	-207.0	46.3	191.3
3	1 st	0.92	30.6	5.2x10 ³	-147	27.9	85	0.91	1.3	2.2x10 ⁻²	-313	-1.5	100.3
	2 nd	0.99	55.9	5.2x10 ⁴	-165	51.6	138	0.98	33.2	3x10 ²	-194	28.8	130.3
	3 rd	0.93	26.2	9.1x10 ⁻¹	-254	19.4	228	0.95	19.4	2x10 ⁻³	-257.7	12.6	224.4
4	1 st	0.90	3.9	3.8x10 ⁻¹³	-485	0.62	193	0.99	5.1	5.5x10 ⁻¹	-291.2	1.84	117.7
	2 nd	0.97	49.9	6.3x10 ³	-176.5	45.7	134	0.96	23.2	1.3x10 ⁻³	-221	19.1	129.8
	3 rd	0.96	68.7	1.8x10 ⁶	-132	62.5	161	0.96	38.8	1.3x10 ²	-236	32.6	209.5
5	1 st	0.91	41.5	1.8x10 ⁵	-145	38.7	87	0.91	19.5	2x10 ²	-238.5	16.6	97.5
	2 nd	0.98	42.5	1.5x10 ⁶	-167	38.4	120	0.98	23.5	3.6x10	-211.4	19.4	123.9
	3 rd	0.96	51.1	4.1x10 ²	-199	46.3	160	0.97	20.5	1x10 ⁻³	-236	15.8	150.7
	4 th	0.99	745.3	4.1x10 ⁴¹	543.7	738.8	310	0.99	346.5	7.1x10 ⁻⁴	183.5	340	195.3
6	1 st	0.92	33.6	5.6x10 ³	-173.9	30.8	88	0.92	13.9	2.5x10 ¹	-257.7	11.16	95.9
	2 nd	0.97	52.0	3.9x10 ⁴	-180	48.4	127	0.96	21.8	5.6x10	-237	18.1	121.4
	3 rd	0.97	188.3	3.7x10 ¹⁶	-14.8	183.8	192	0.97	88	3.1x10 ⁷	-121	83.2	152.7
	4 th	0.97	44	5.6x10 ⁷	-104	37.7	117	0.98	29	6.2x10 ⁻⁴	-238	22.7	204.3
	5 th	0.98	169	6.8x10 ⁸	-84.7	161.7	235	0.97	77.8	2.7x10 ⁻⁶	-182.4	70.6	230.2

3.7. Optical Properties

To clarify the conductivity of the isolated complexes, the optical band gap energy (E_g) of azo-ligand and its complexes have been calculated from the following equations [59 - 61]:

The measured transmittance (T) was used to calculate approximately the absorption coefficient (α) using the relation

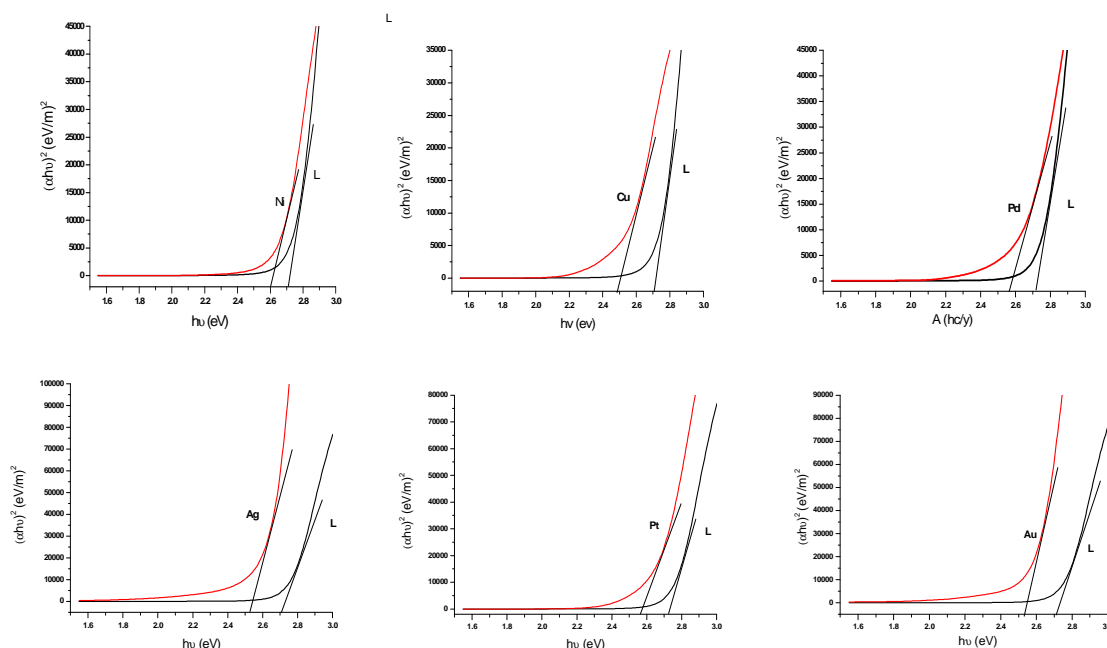
$$\alpha = 1/d \ln(1/T)$$

where d is the width of the cell, T is the measured transmittance. The optical band gap was estimated using Tuac's equations:

$$ch\nu = A (h\nu - E_g)^m$$

where m is equal to 1/2 and 2 for direct and indirect transition, respectively, A is an energy independent constant.

The values of α calculated from the first equation was used to plot $(\alpha h\nu)^2$ vs. $h\nu$ (Fig. 5) from which an indirect band gap was found by extrapolating the linear portion of the curve to $(\alpha h\nu)^2 = 0$. The values of indirect optical band gap E_g were determined and given in Table 1. The E_g values of azo-ligand and its complexes were found to be at 2.72 and 2.53 - 2.60 eV, respectively as indicated in Fig. 6 and Table 1 revealed higher E_g vales of ligand compared with their corresponding complexes. As reported in literature [62] it is suggested that after complexation, metal leads to raise mobilization of the ligand electrons by accepting them in its shell. It can be evaluated that after formation of the complexes, the chemical structure of the ligand is changed, the width of the localized levels is expanded and in turn, the band gap is smaller. This result is very significant in applications of electronic and optoelectronic devices, because of the lower optical band gap of the materials [63]. Worthy mention, small band gap facilitates electronic transitions between the HOMO - LUMO energy levels and makes the molecule more electro-conductive [64]. The obtained band gap values suggest that these complexes are semiconductors and lie in the same range of highly efficient photovoltaic materials. So, the present compounds could be considered potential materials for harvesting solar radiation in solar cell applications [62, 65]. The little difference in the optical band gap E_g values between all studied complexes may be due to their synonymous chemical structures.



Figs. 5: The plots of $(\alpha h\nu)^2$ vs. $h\nu$ of ligand and its metal complexes

3.8. Anticancer activity

The Azo-dye compounds might have promising potential anticancer applications, since these ligand can lead to possible alternative modes of cytotoxic action, such as intercalative DNA lesion [67, 68], square-planar metal complexes with aromatic ligands bind to DNA by intercalation [69]. The cytotoxicity activities of gold complex were tested against (MCF-7) human tumor cell lines. The reported results in terms of IC_{50} value for it is 48 $\mu\text{g/ml}$ **Fig. 6**: For comparison purposes, the cytotoxicity of cisplatin, as standard antitumor drug, was evaluated and produced IC_{50} value (0.426 $\mu\text{g/ml}$) under the same conditions. As depicted the complex has noticeable cytotoxicity activation, also these finding could be explained by the solubility effect as fairly good relationship could be seen between activity and solubility of the compounds. The activity of the gold complex could be explained by its greater solubility and lipophilicity. The lipophilicity increases with increasing bulkiness and may facilitate transport through the cellular membrane [70].

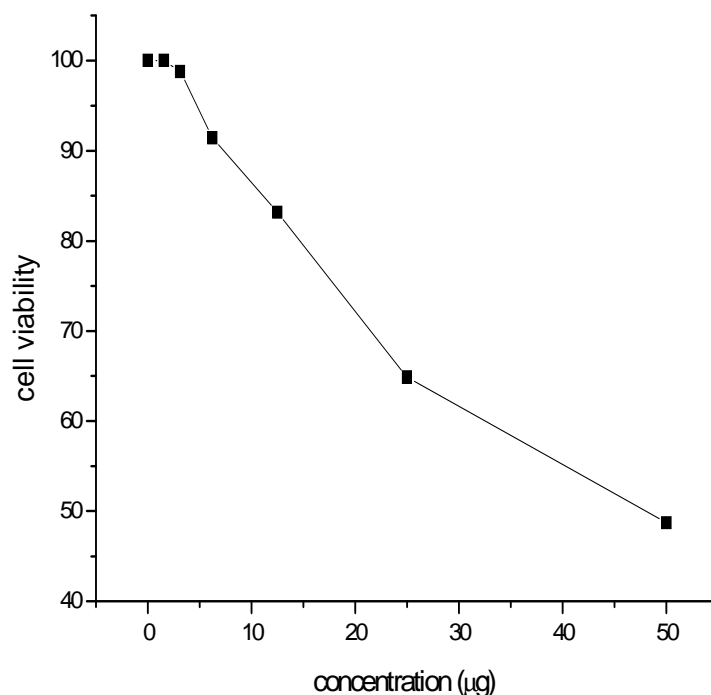


Fig. 6: Cytotoxicity of Au (II) complex

CONCLUSION

A series of metal-azo complexes derived from some selected Azo-ligand have been isolated in pure form. The ligand and their solid metal complexes may be prepared by conventional reflux method. Comparison of the elemental analysis for both calculated and found percentages indicates that the compositions of the isolated solid complexes coincide well with the proposed formulae. Elemental analyses (C, H, N and M%), (FT-IR, UV-Vis and ESR) spectroscopy, thermal measurement and magnetism besides the difference in the color between the free ligand and its corresponding complexes evidenced the formation of the desired azo complexes. The synthesized metal complexes possessed a tetrahedral geometry for [Cu (II), Ni (II)], square planer [Pd (II), Pt (IV)] and Au (III) and trigonal geometry for Ag(I) metal ion. The indirect band gap energies (Eg) for the ligand and complexes lay in the range of semiconductor materials. The investigated azo-gold complex were assayed for their anti-tumor activities against the human breast cancer cell line. The results suggested that the Au(III)-complexes have growth inhibition activity.

REFERENCES

- [1] A Afkhami; M Bahram; *Spectrochim. Acta* **2004**, 60 (A),181.
- [2] H Bock; K Wittle; M Veit; N Wiberg; *J. Am. Chem. Soc.* **1976**, 98, 109
- [3] KM Patel; VH Patel; MP Patel; RG Patel; *Dyes Pigments* **2002**, 55, 53.
- [4] SA Ibrahim; AM Hammam; AM Kamal El-Dean; AA Mohamed; NN Rageh; *Can. J. Appl. Spectrosc.* **1993**, 38, 1.
- [5] M Sefkow; H Kaatz; *Tetrahedron Lett.* **1999**, 40, 6561;
- [6] P Chen Tsai; L Jing Wang; *Dyes Pigments* **2005**, 64, 259.
- [7] M Gaber; MM Ayad; YS Elsayed; *Spectrochim. Acta* **2005**, 62,694.
- [8] J Matijevic-Sosa; M Vinkovic; Vikie-Topic; D. *Croat. Chem. Acta*, **2006**, 79, (3),489-495.
- [9] J Costamagna; J Vargas; R Latorre; A Alvarado; Mena, G. *Coord. Chem. Rev.*, **1992**, 119, 67-88.
- [10] SS Kandil; SMA Katib; NHM Yarkandi, *Trans. Met. Chem.* **2007**, 32, 791-798.
- [11] HTY Fahmy; SAF Sherif Rostom; AA Bekhit; *Arch. Pharm. Pharm. Med. Chem.* **2002**, 5, 213-222.
- [12] MN Nasr; MM Gineinah, *Arch. Pharm.*, **2002**, 335, 289-295.
- [13] B Tozkoparan; M Ertan; P Kelicen; R Demirdamar, *Il Farmaco*, **1999**, 54,588-593.
- [14] EA Amr; MM Ashraf; FM Salwa; AA Nagla; AG Hammam, *Bioorgan. Med. Chem.* **2006**, 14, 5481-5488.
- [15] N Kumar; G Singh; Yadav, A. K. *Heteroat. Chem.* **2001**, 12, 52-56.

- [16] G Mangalagiu; M Ungureanu; G Grosu; I Mangalagiu; Petrovanu, M. *Ann. Pharm. Fr.* **2001**, 59, 139-140.
- [17] Gardenghi, D. *Inorg. Chem.* **2007**, 515, 1-7.
- [18] M Sonmez; CM elebi; A Levent; I Berber; S, ZJ ent`urk; *Coord. Chem.* **2010** ,63,848-860.
- [19] TR Chen; JD Chen; TC Keng; JC Wang, *Tetrahedron Lett.* **2001**, 42, 7915-7917.
- [20] L Prog Akcelrud, *Polym. Sci.* **2003**, 28, 875-962.
- [21] H Wang; N Song; Li, H.; Li, Y.; Li, X. *Synthetic Met.* **2005**, 151, 279-284.
- [22] M Carrard; S Goncalves-Conto; L Si-Ahmed; D Ades; A Siove, *Thin Solid Films* **1999**, 352, 189-194.
- [23] L Feng; Z Chen, *Polymer* **2005**, 46, 3952-3956.
- [24] Q Fang; A Tanimoto; T Yamamoto, *Synthetic Met.* **2005**, 150, 73-78.
- [25] C Qin; X Wang; E Wang; C Hu; L Xu, *Inorg. Chim.,Acta.* **2004**, 357, 3683-3688.
- [26] A Heller; EJ Wasserman, *Chem. Phys.* **1965**, 42, 949-956.
- [27] CF Shaw III; *Chem. Rev.* **1999**, 99, 2589-2600.
- [28] GD Champion; GG Graham; JB Ziegler; *Baillieres Clin. Rheumatol.* **1990**, 4, 491-534.
- [29] SP Fricker; *Gold Bull.* **1996** 29, 53-59.
- [30] ERT Tiekink; *Crit. Rev. On col.Hematol.* **2002**, 42, 225-248.
- [31] ERT Tiekink; *Gold Bull.* **2003**, 36, 117-124.
- [32] C Gabbiani; A Casini; L Messori; *Gold Bull.* **2007**, 40,73-81.
- [33] L Messori; G Marcon; A Innocenti; E Gallori; M Franchi; P. Orioli, *Bioinorg. Chem. Appl.* **2005**, 3, 239-253.
- [34] PG Baraldi; MG Pavani; M Nunez; P Brigidi; B Vitali; Gambari; Romagnoli; R. *Bioorg. Med. Chem.* **2002**, 10,449-456.
- [35] MN Nasr; MM ineinah, *Arch. Pharm.* **2002** ,335, 289-295.
- [36] S Leistner; G Wagner; M Guetscharo; E Glusa, *Pharmazie* **1986**, 41, 54-55.
- [37] E Bousquet; G Romero; F Guerrera; A Caruso; MA Roxas, *Farmaco Ed. Sci.* **1985**, 40, 869-874.
- [38] N Kumar; G Singh; Yadav, A. K. *Heteroat. Chem.* **2001**, 12, 52-56.
- [39] G Mangalagiu; M Ungureanu; G Grosu; Mangalagiu, I.; Petrovanu, M. *Ann. Pharm. Fr.* **2001** ,59, 139-140.
- [40] A.I.Vogel, A text Book of Quantitative Inorganic Analysis, Longman, fourth ed., London, (**1989**).
- [41] AA El-Kateb.; NM Abd El-Rahman.; TS Saleh; Ali M. Hassan; AS El haddad and AY El-Dosoky, *J. Nature and Science* **2012**, 11, 10.
- [42] T Mosman; *J.Immunol.Methods.* **1983**, 65, 55
- [43] N Kabay; E Erdem; R Kilincarslan and E Yilidirim; *Transition Met.Chem.*, **2007**, 32, 1068.
- [44] BS Creaven; M Devereux; A Foltyn; S Mc Clean; G Rosair; VR Thangella; M Walsh, *j Polyhedron* **2010**, 29, 813-822.
- [45] KD Miskra; R Rai; OP Pandey; SK Sengupta, *Transition Met. Chem.* **1992**, 17, 127.
- [46] GG Mohamed; *Spectrochimica Acta, Part A.* **2001**, 57, 411.
- [47] SS Kandil; SMA Katib; NHM Yarkandi, *Trans. Met. Chem.* **2007**, 32, 791-798.
- [48] R Gup and B Kirikan; *j Spectrochimca Acta* **2006**, 64, 809-815
- [49] R Kilincarslan and E Erem; *Transition Met. Chem.* **2007**, 32,102.
- [50] GL Eichhorn; JC Bailar; J.Am.Chem.Soc. **1953**, 75, 2905.
- [51] M Levitt, Spin Dynamics: *Basics of Nuclear Magnetic Resonance*, (John Wiley and Sons), **2001**.
- [52] D Kivelson, R Neiman, *J. Chem. Phys.* **1961**, 35, 149.
- [53] ABP Liver, Inorganic electronic spectroscopy, Elsevier, New York, **1984**.
- [54] D Kivelson, R Nieman, *J. Chem. Phys.* **1961**, 35,149-155.
- [55] AW Coats; JP Redfern, *Nature* **1964**, 20, 68.
- [56] HH Horowitz; G Metzger, *J Anal Chem* **1963**, 35,1464.
- [57] T Moeller, *J Inorg Chem* **1972**, 2, 282.
- [58] T Gangaldevi; K Muraleedliaran; M Kannan, *J Thermo Acta.* **1991**, 191, 105.
- [59] XT Tao; H Suzuki; T Watanabe; SH Lee; S Miyata; H Sasabe; *Appl. Phys. Lett.*, **1997**, 70, 1503-1505.
- [60] MM Rashad; AM Hassan; AM Nassar; NM Ibrahim; A Mourtada; *Appl. Phys., A* **2013**, 117, 877-890.
- [61] MM Rashad; AO Turkey; AT Kandil; J. Mater. Sci.: *Mater. Electron.*, **2013**, 24, 3284-3291.
- [62] F Karipcin; B Dede; Y Caglar; D Hur; S Ilcan; M Caglar; Y Sahin; *Opt. Commun.*, **2007**, 272, 131-137.
- [63] N Turan; B Gündüz; H Korkoca; R Adigüzel; N Çolak; K Buldurun; *J. Mex. Chem. Soc.*, **2014**, 58(1), 65-75.
- [64] SK Sengupta; OP Pandey; BK Srivastava; V Sharma; *Transit. Met. Chem.*, **1998**, 23, 349-353.
- [65] ML Fu; GC Guo; X Liu; LZ Cai; JS Huang; *Inorg. Chem. Commun.*, **2005**, 8, 18-21.
- [66] JI Gittleman; EK Sichel; Y Arie; *Sol. Energy Mater.*, **1997**, 1, 93-104.
- [67] AS Abu-Surrah; M Kettunen; *Curr. Med. Chem.*, **2006**, 13, 133.
- [68] C Bincoletto; ILS Tersariol; CR Oliveira; S Dreher; DM Fausto; MA Soufen; FD Nascimento; ACF Caires; *Bioorg. Med. Chem.*, **2005**, 13, 3047.
- [69] G Marverti; M Cusumano; A Ligabue; ML Di Pietro; PA Vainiglia; A Ferrari; MS M. Bergomi; Moruzzi; C Frassinetti; *J. Inorg. Biochem.* **2008**, 102, 699.
- [70] J Reedijk; *Chem. Commun.*, **1996**, 801.